NASA TECHNICAL NOTE

NASA TN D-2045

c. 1

NASA TN D-2045

RESIDUAL STATIC STRENGTH OF SEVERAL TITANIUM AND STAINLESS-STEEL ALLOYS AND ONE SUPERALLOY AT -109° F, 70° F, AND 550° F

by I. E. Figge

Langley Research Center
Langley Station, Hampton, Va.

NATIONAL AERONAUTICS AND SPACE ADMINISTRATION • WASHINGTON, D. C. • DECEMBER 1963

RESIDUAL STATIC STRENGTH OF SEVERAL TITANIUM AND STAINLESS-STEEL ALLOYS AND ONE SUPERALLOY AT -109° F, 70° F, AND 550° F

By I. E. Figge

Langley Research Center
Langley Station, Hampton, Va.

NATIONAL AERONAUTICS AND SPACE ADMINISTRATION

RESIDUAL STATIC STRENGTH OF SEVERAL TITANIUM AND STAINLESS-STEEL ALLOYS AND ONE SUPERALLOY AT -109° F, 70° F, AND 550° F

By I. E. Figge

SUMMARY

Residual static-strength tests were conducted on 8-inch-wide sheet specimens containing central fatigue cracks of various lengths at -109° F, 70° F, and 550° F. The materials investigated were: Ti-4Al-3Mo-1V (aged), Ti-6Al-4V (annealed), Ti-8Al-1Mo-1V (annealed), Ti-8Al-1Mo-1V (triplex annealed), AM 350 (20% CRT), AM 350 (double aged), PH 15-7Mo (TH 1050), AISI 301 (50% CR), and René 41 (condition B). When compared on a residual-strength—density basis, the titanium alloys, in general, and the alloy Ti-8Al-1Mo-1V (triplex annealed), in particular, appear to demonstrate the most favorable residual static-strength properties of the materials tested. Analysis of the data by the use of unified notch-strength analysis method of NASA TN D-1259 is discussed.

INTRODUCTION

Information is needed to aid in the selection of new structural materials for use in supersonic aircraft construction. Because of the operational requirements of these aircraft, materials will be required which can maintain their integrity throughout a large range of temperatures.

One of the most important considerations in selecting an aircraft structural material is its static-strength properties in the presence of a crack (residual static strength). If the strength of a material is reduced too severely when a crack exists, the structure may fail before corrective action can be taken.

The purpose of this investigation was to determine the residual static strengths of several titanium and stainless-steel alloys and one superalloy at -109° F, 70° F, and 550° F. The materials are among the candidate materials for the primary structure of a supersonic commercial air transport and the temperatures selected simulate approximately the temperature range encountered by a Mach 3 aircraft. (See ref. 1.) The experimental results were analyzed by using the unified notch-strength analysis method. (See refs. 2 and 3.)

SYMBOLS

a	half-length of internal notch, in.
E	modulus of elasticity, ksi
$E_{s,n}$	secant modulus corresponding to net-section stress, ksi
$E_{s,u}$	secant modulus corresponding to stress at ultimate load, ksi
e	elongation in 2-inch gage length, percent
K_u	static notch-strength factor
S_n	tensile strength of notched specimen (based on net section before loading starts), ksi
w	width of specimen, in.
ρ'	material constant (Neuber constant), in.
σ_u	ultimate tensile strength, ksi
σ_y	yield strength (0.2-percent offset), ksi

MATERIALS AND SPECIMENS

For each specific alloy, all material used in this investigation was obtained from the same mill heat. Subsequent heat treating was done at the Langley Research Center on Ti-4Al-3Mo-1V, AM 350, PH 15-7Mo, and René 41. The remainder of the material was tested in the as-received condition. Details of the heat treatments are presented in table I. All phases of heat treating, machining, and handling followed rigid quality control specifications established at Langley. The tensile properties of the materials tested are given in table II. Each result quoted in table II is the average of at least three tests.

The specimen configuration used in the residual static-strength tests is shown in figure 1. Sheet specimens 8 inches wide and 24 inches long were used. The titanium-alloy specimens were nominally 0.040 inch thick with the exception of the Ti-8Al-1Mo-1V (triplex annealed) specimens which were nominally 0.050 inch thick. The stainless-steel and superalloy specimens were nominally 0.024 inch thick. The grain direction was parallel to the direction of loading. A crack starter in the form of a 0.01-inch-wide slit was cut by a spark-discharge technique in the center of each specimen perpendicular to the direction of loading. (See fig. 1.)

A crack-propagation investigation (not presented in this paper) was conducted on approximately two-thirds of the specimens prior to the determination of residual static strength. Cracks were grown at various stress levels for the crack-propagation study at both 70° F and 550° F until they were within approximately 0.2 inch of the desired length for the static tests. To prepare the specimens for the residual static-strength study, the stress range was changed to 0 to 27 ksi for the titanium alloys and 0 to 40 ksi for the stainless steels and superalloy. The cracks were then grown at these new stress levels at 70° F until the desired crack lengths were obtained. This procedure was followed to produce a consistent influence of prior stress of the material immediately ahead of the crack tip. The specimens which had cracks grown at 70° F and 550° F for the crack-propagation investigation were then tested statically at 550° F and -109° F, respectively. The specimens that were not included in the crack-propagation investigation had cracks grown to their full length at 70° F at the specific stress ranges previously indicated. These specimens were tested statically at 70° F.

EQUIPMENT AND TEST PROCEDURE

A 120,000-pound capacity hydraulic jack was used to perform the static tests. A detailed description of this machine is given in reference 4. A load rate of 30,000 pounds per minute was used on all tests. The maximum load at failure was obtained from a load-indicating system which is an integral part of the testing machine.

During the static tests all specimens with the exception of three Ti-8Al-1Mo-1V (annealed) specimens and three PH 15-7 Mo specimens were restrained from buckling in the test section by means of guide plates. The specimens tested at 70° F (room temperature) were clamped between lubricated guides similar to those described in reference 5. A clear plastic window was installed in the guide to facilitate inspection of the specimen during the static test. The room-temperature test setup is shown in figure 2(a).

Temperatures of -109° F were obtained by clamping a block of dry ice approximately 8 inches by 10 inches by $1\frac{1}{2}$ inches on each side of the test section. These blocks also served as the guide plates. Thermocouples spotwelded to the specimen and connected to a strip-chart recorder were used to monitor the temperature. The specimen temperature was found to be uniform throughout the test section within 2°. The cryogenic test setup is shown in figure 2(b).

Temperatures of 550° F were obtained by clamping a sandwich consisting of an insulating block, an electrical-resistance-type ceramic heating slab, and a graphite block to each side of the test section. The graphite blocks served as the guides in this case. The specimen temperature was regulated by means of a saturable reactor temperature controller and was found to be uniform throughout the test section within ±5°. The specimens were brought up to temperature and held for approximately 5 minutes prior to static testing. The elevated-temperature test setup is shown in figure 2(c).

RESULTS AND DISCUSSION

The experimental results of the residual static-strength tests are presented in table III and in figures 3 to 11. The residual static strength (based on the net section before loading starts) S_n is plotted against $2a/w$ at -109° F, 70° F, and 550° F.

Analysis by Unified Notch-Strength Method

The results obtained from the static tests were analyzed by using the unified notch-strength analysis method. (See refs. 2 and 3.) Details of the calculations used are given in the appendix of this report. Tentative Neuber constants $\sqrt{\rho'}$ required in the calculations have been previously developed for the titanium alloys. (See ref. 3.) For convenience, curves of these values are reproduced in figure 12.

Analysis of the present data on the α-phase titanium alloys, Ti-8Al-1Mo-1V (annealed) and Ti-8Al-1Mo-1V (triplex annealed), suggests that the criterion (that is, material phase) used in reference 3 to distinguish the $\sqrt{\rho'}$ curves is questionable. Use of the α-curve resulted in predictions which fit the experimental data reasonably well for the Ti-8Al-1Mo-1V (annealed) material. (See fig. 5.) However, use of the same curve for the Ti-8Al-1Mo-1V (triplex annealed) material resulted in extremely poor agreement. (See fig. 6.) The αβ-curve was used and, as a result, a considerably improved fit to the data was obtained. (See fig. 6.) On the basis of these observations, it appears that two distinct $\sqrt{\rho'}$ curves are required for the titanium alloys, but the choice of the appropriate curve should not be based solely on the material phase but should also include some additional parameters. At the present, these parameters are not clearly defined.

Complete curves of $\sqrt{\rho'}$ plotted against σ_u have not been developed for the stainless-steel alloys and superalloy as yet. The values of $\sqrt{\rho'}$ used in this investigation for these materials were adjusted in such a way that the theory would give a reasonable fit to the present data.

Some of the values of $\sqrt{\rho'}$ (for example, those for Ti-4Al-3Mo-1V (aged), AM 350 (20% CRT), and PH 15-7Mo (TH 1050) at 550° F) were unusually large. Although the theory fits the data reasonably well if these large values of $\sqrt{\rho'}$ are used, it should be remembered that the theory assumes that ρ' is a constant which has been interpreted as an "effective radius." Effective radii as large as 41.3 inches (AM 350 (20% CRT) at 550° F) do not appear to be reasonable. Even values of ρ' equal to 0.792 inch and 0.798 inch (Ti-4Al-3Mo-1V (aged) and PH 15-7Mo (TH 1050), respectively, at 550° F) are of such magnitude that their validity becomes questionable. Some insight may be gained in understanding the cause of these excessive values of ρ' by examining the simplifying assumptions used in the development of the unified analysis method. The method assumes that:

(1) the plastic correction factor, as expressed by $\frac{E_{s,u}}{E_{s,n}}$ is generally valid

(2) the slow crack growth that generally precedes final fracture can be ignored

(3) the material remains metallurgically stable throughout the test

(4) the static failure can be characterized by the nominal ultimate tensile strength.

The empirical adjustment of ρ' must account for all factors not adequately handled by these assumptions.

Observations on Individual Materials

In this section, the results of residual-static-strength tests at -109° F and 550° F are compared with the results of tests conducted at 70° F. In all cases there was a substantial reduction in the ultimate strength with increasing temperature whereas in most cases there was little change in the residual strength. A brief discussion of the agreement between theory and experimental results is given for each of the titanium alloys. The values of $\sqrt{\rho'}$ used in the analysis are presented in the figures.

Ti-4Al-3Mo-1V (aged).- The values of residual strength for Ti-4Al-3Mo-1V (aged) remain virtually unchanged over the temperature range. (See fig. 3.) The predicted and experimental values are in good agreement at the three test temperatures.

Ti-6Al-4V (annealed).- The values of residual strength for Ti-6Al-4V (annealed) are slightly lower at -109° F and 550° F than at 70° F. (See fig. 4.) The value of residual strength in one case exceeds the ultimate strength at 550° F. No explanation is offered for this phenomenon. The theory is in good agreement with the test data at -109° F and in fair agreement at 70° F. At 550° F, the theory is in poor agreement but is conservative.

Ti-8Al-1Mo-1V (annealed).- Again as in the case of Ti-6Al-4V (annealed), the values of residual strength for Ti-8Al-1Mo-1V (annealed) are slightly lower at -109° F than at 70° F. (See fig. 5.) It is interesting to note that the values of residual strength are somewhat higher at 550° F than at either 70° F or -109° F. Other investigators have also noted an increase in residual strength at elevated temperatures for this material. (See ref. 1.) If the $\sqrt{\rho'}$ curve for the α-alloys is used, the agreement between predicted values and experimental values is good at -109° F and fair at 70° F and 550° F.

Ti-8Al-1Mo-1V (triplex annealed).- The values of residual strength for Ti-8Al-1Mo-1V (triplex annealed) remain essentially the same at -109° F as those at 70° F. (See fig. 6.) The residual strength was reduced slightly at 550° F. This material demonstrated significantly higher values of residual strength than Ti-8Al-1Mo-1V (annealed) at both -109° F and 70° F. At 550° F, Ti-8Al-1Mo-1V (annealed) had slightly higher values of residual strength than the triplex annealed material. If the $\sqrt{\rho'}$ curve for the αβ-alloys is used as discussed previously, the theory fits the data rather poorly at -109° F. At both 70° F and 550° F the agreement is very good.

AM 350 (double aged).- At -109° F, AM 350 (double aged) behaves in a brittle fashion. (See fig. 7.) The test specimens shattered into several pieces at failure. (See fig. 13(a).) This brittle behavior is associated with the very low values of residual strength (approximately one-third of the values at 70° F). The strength of this material is slightly lower at 550° F than at 70° F.

AM 350 (20% CRT).- At -109° F, the residual strength of AM 350 (20% CRT) was slightly lower than at 70° F. (See fig. 8.) At 70° F, an interesting phenomenon occurred. The material demonstrated a completely ductile mode of failure; that is, there was no evidence of any rapid fracture as is normally experienced in most high-strength materials. Figure 13(b) presents a typical failed specimen. There was a large amount of necking and Lüders lines were evident. At 550° F, there was a small reduction in strength compared with the values at 70° F. It is interesting to note that this material had a very low value of elongation (2.7 percent) at 550° F. If this value was taken at face value, it would be anticipated that this material should be very notch sensitive; however, in reality, it is very notch insensitive. It can be seen from figure 8 that three test points are equal to or higher than the ultimate tensile strength and the remainder of the data are only slightly below it. Metallurgical examination of the material in the vicinity of the fatigue crack tip of these specimens revealed an increase in the martensitic content. This transformation is believed to have occurred mainly during the fatigue cycling of the specimen as a direct result of cyclic strain. Other investigators have noted a martensitic transformation in AM 350 due to straining. (See ref. 1.) This transformation essentially produces a new material in the vicinity of the crack tip which has properties superior to those of the virgin material. Apparently, the elevated temperature has a considerably more deleterious effect on uncycled material (from which the ultimate tensile strength is obtained) than it does on the transformed material. The unusually large value of $\sqrt{\rho'}$ $\left(\text{that is, } 6.42 \text{ inches}^{1/2}\right)$ can probably be attributed to the fact that this material is metallurgically unstable and thereby violates one of the assumptions used in the development of the analysis method. (See section on analysis by unified notch-strength method.)

AISI 301 (50% CR).- The values of residual strength for AISI 301 (50% CR) are somewhat higher at -109° F than at 70° F. (See fig. 9.) This increase in strength might be explained by the fact that the elongation of AISI 301 is approximately six times larger at -109° F than at 70° F. At 550° F, the residual strength is reduced to approximately one-half its value at 70° F. Work at Langley indicates this severe reduction in strength is probably due to embrittlement which is caused by the fine precipitates which form at these temperatures.

PH 15-7Mo (TH 1050).- As in AM 350 (double aged), a brittle mode of failure was evident at -109° F for PH 15-7Mo (TH 1050). (See fig. 10.) In this case the specimens not only shattered into several pieces but also had a pronounced saw-tooth type of failure. (See fig. 13(c).) Again very low values of residual strength were obtained. There is no evidence from the tensile properties that this phenomenon might be expected. At 550° F, the values of residual strength are approximately equal to the 70° F test results.

René 41 (condition B).- The values of residual strength of René 41 (condition B) were somewhat lower at -109° F than at 70° F. At 550° F they were approximately equal to the 70° F results.

Strength-Density Comparisons

A plot of the residual static strengths divided by density is presented in figure 14. The data were normalized by dividing the residual strengths of each material by their respective densities. Figure 14 presents these results at -109° F, 70° F, and 550° F. The values of residual strength used in this figure were obtained from fairings through the actual test data rather than from the predicted results.

From this figure it appears that, in general, the titanium alloys have higher ratios of residual strength to density than the stainless-steel alloys and the superalloy. It also appears that Ti-8Al-1Mo-1V (triplex annealed) exhibits the best overall residual static-strength properties of the materials tested.

SUMMARY OF RESULTS

Residual static-strength tests were conducted on 8-inch-wide sheet specimens containing central fatigue cracks of various lengths at -109° F, 70° F, and 550° F and the following results were obtained:

1. On a residual-strength—density basis, the titanium alloys appear to be superior to either the stainless steels or superalloy.

2. On a residual-strength—density basis, Ti-8Al-1Mo-1V (triplex annealed) demonstrates the most favorable properties over the temperature range investigated.

3. In general, the reduction in ultimate tensile strength with increasing temperature is considerably higher than the reduction in the residual static strength.

4. AM 350 (double aged) and PH 15-7Mo (TH 1050) demonstrated a brittle mode of failure at -109° F.

5. AM 350 (20% CRT) demonstrated a completely ductile mode of failure at 70° F.

6. Slight notch-strengthening occurred in AM 350 (20% CRT) at 550° F for short cracks.

7. The strength of AISI 301 (50% CR) was considerably less at 550° F than at 70° F.

Langley Research Center,
National Aeronautics and Space Administration,
Langley Station, Hampton, Va., September 6, 1963.

APPENDIX

METHOD OF CALCULATION

The following is a brief description of the method used to calculate the residual static strength of a sheet specimen containing a fatigue crack. A detailed description of the analysis method can be found in references 2 and 3.

The theoretical stress concentration factor for a sheet specimen containing a fatigue crack is given by the formula

$$K_{TN} = 1 + 2K_w\sqrt{\frac{a}{\rho'}}$$

where $K_w = \sqrt{\frac{1 - \frac{2a}{w}}{1 + \frac{2a}{w}}}$ (from ref. 6), a is one-half the crack length, w is the specimen width, and $\sqrt{\rho'}$ is the Neuber constant obtained from figure 12. The theoretical factor K_{TN} is then corrected for plasticity by the formula

$$K_u = 1 + \left(K_{TN} - 1\right)\frac{E_{s,u}}{E_{s,n}}$$

where $E_{s,u}$ is the secant modulus corresponding to the stress at the ultimate load and $E_{s,n}$ is the secant modulus corresponding to the net-section stress. For net-section stresses below the proportional limit $E_{s,n}$ is by definition equal to Young's modulus E. In this report E was also substituted for $E_{s,n}$ for net-section stresses above the proportional limit in order to improve the fit to the data. Since the complete stress-strain curves (up to failure) were not available, the values of $E_{s,u}$ were estimated by the formula

$$E_{s,u} = \frac{E}{1 + \frac{0.8eE}{\sigma_u}}$$

where e is the elongation in a 2-inch gage length, E is the elastic (Young's) modulus, and σ_u is the ultimate tensile strength. Finally, the residual static strength S_n based on the net section existing at start of test, is given by the formula:

$$S_n = \frac{\sigma_u}{K_u}$$

REFERENCES

1. Raring, Richard H., Freeman, J. W., Schultz, J. W., and Voorhees, H. R.: Progress Report of the NASA Special Committee on Materials Research for Supersonic Transports. NASA TN D-1798, 1963.

2. Kuhn, Paul, and Figge, I. E.: Unified Notch-Strength Analysis for Wrought Aluminum Alloys. NASA TN D-1259, 1962.

3. Kuhn, Paul: Notch Effects on Fatigue and Static Strength. Paper presented at Symposium on Aeronautical Fatigue sponsored by ICAF and AGARD (Rome, Italy), Apr. 1963.

4. Illg, Walter: Fatigue Tests on Notched and Unnotched Sheet Specimens of 2024-T3 and 7075-T6 Aluminum Alloys and of SAE 4130 Steel With Special Consideration of the Life Range From 2 to 10,000 Cycles. NACA TN 3866, 1956.

5. Brueggeman, W. C., and Mayer, M., Jr.: Guides for Preventing Buckling in Axial Fatigue Tests of Thin Sheet-Metal Specimens. NACA TN 931, 1944.

6. Dixon, J. R.: Stress Distribution Around Edge Slits in a Plate Loaded in Tension - The Effect of Finite Width of Plate. Jour. R.A.S. (Tech. Notes), vol. 66, no. 617, May 1962, pp. 320-322.

TABLE I.- MATERIAL HEAT TREATMENTS

Material	Condition	Heat treatment
Ti-4Al-3Mo-1V	Aged	1650° F for 20 minutes, water quenched, 1050° F for 4 hours, air cooled
Ti-6Al-4V	Annealed (mill)	1475° F for 1 hour, furnace cooled to 1300° F, air cooled
Ti-8Al-1Mo-1V	Annealed (mill)	1450° F for 8 hours, furnace cooled
Ti-8Al-1Mo-1V	Triplex annealed	1450° F for 8 hours, furnace cooled, 1850° F for 5 minutes, air cooled, 1375° F for 15 minutes, air cooled
AM 350	Double aged	Received in condition H; 1375° F for 3 hours, air cooled to 80° F maximum, 850° F for 3 hours, air cooled
AM 350	20% CRT	20% cold roll, aged in hot caustic at 930° F for 3 to 5 minutes
AISI 301	50% CR	52% cold roll
PH 15-7Mo	TH 1050	1400° F for 90 minutes, cool to 60° F within 1 hour, hold 30 minutes, heat to 1050° F for 90 minutes, air cooled
René 41	Condition B	1950° F for 3 hours, air cooled, 1400° F for 16 hours, air cooled

TABLE II.- AVERAGE TENSILE PROPERTIES OF MATERIALS TESTED

[Grain direction longitudinal]

Temperature, °F	σ_u, ksi	σ_y, ksi	E, ksi	e, percent (2-in. gage)	Number of tests
		Ti-4Al-3Mo-1V (aged)			
-109	164.3	143.2	16.0×10^3	12.5	5
70	139.1	120.0	15.5	10.7	5
550	102.0	88.0	14.6	7.3	3
		Ti-6Al-4V (annealed)			
-109	170.8	163.0	17.4×10^3	13.2	5
70	144.4	137.3	16.4	12.5	5
550	109.1	96.7	14.4	7.5	5
		Ti-8Al-1Mo-1V (annealed)			
-109	176.0	171.0	19.3×10^3	19.0	5
70	156.2	145.7	18.0	18.5	5
550	120.3	103.5	16.0	14.3	3
		Ti-8Al-1Mo-1V (triplex annealed)			
-109	178.6	161.8	18.3×10^3	15.0	4
70	153.3	140.0	18.2	13.6	5
550	120.0	98.0	16.0	11.0	3
		AM 350 (double aged)			
-109	211.7	178.0	30.1×10^3	19.0	5
70	186.0	154.9	28.5	16.0	5
550	165.3	124.0	27.8	7.1	3
		AM 350 (20% CRT)			
-109	251.4	175.2	28.9×10^3	19.0	5
70	204.5	182.3	28.6	18.8	5
550	158.3	154.7	27.9	2.7	4
		AISI 301 (50% CR)			
-109	234.8	203.7	29.5×10^3	29.0	5
70	212.0	189.7	25.6	5.0	5
550	178.6	149.3	23.2	2.6	3
		PH 15-7Mo (TH 1050)			
-109	219.3	209.5	30.8×10^3	10.0	5
70	199.9	195.0	29.2	8.5	5
550	179.2	177.3	24.8	3.0	3
		René 41 (condition B)			
-109	201.0	143.2	31.0×10^3	17.8	3
70	189.8	138.3	30.8	17.5	3
550	171.5	133.4	30.3	9.5	3

TABLE III.- RESIDUAL STATIC-STRENGTH TEST RESULTS

Temperature, °F	2a/w	S_n, ksi
Ti-4Al-3Mo-1V (aged)		
-109	0.110	109.1
-109	.138	104.2
-109	.183	97.7
-109	.252	93.2
-109	.375	86.0
-109	.627	81.3
70	.063	111.2
70	.125	99.6
70	.192	92.1
70	.250	85.7
70	.376	84.3
70	.502	94.6
70	.626	84.5
550	.031	97.3
550	.121	94.0
550	.250	93.7
550	.379	92.0
550	.621	91.7
Ti-6Al-4V (annealed)		
-109	0.106	113.1
-109	.130	108.2
-109	.193	94.7
-109	.250	98.1
-109	.382	76.7
-109	.555	79.4
-109	.605	85.0
70	.060	134.1
70	.119	123.0
70	.194	118.4
70	.252	105.1
70	.379	98.5
70	.506	95.5
70	.628	97.4
550	.031	115.0
550	.071	109.1
550	.119	107.6
550	.158	108.1
550	.253	107.8
Ti-8Al-1Mo-1V (annealed)		
-109	0.115	65.0
-109	.147	66.0
-109	.185	59.3
-109	.315	51.6
-109	.457	53.8
-109	.630	66.2
70	.051	[a]101.0
70	.109	[a]81.5
70	.184	[a]71.5
70	.250	68.8
70	.297	66.2
70	.300	68.5
70	.309	70.4
70	.446	71.5
70	.605	70.9
70	.799	64.0
70	.805	79.5
550	.105	111.7
550	.165	113.2
550	.187	112.4
550	.253	111.3
550	.314	109.9
550	.442	108.6
550	.627	108.0
Ti-8Al-1Mo-1V (triplex annealed)		
-109	0.033	155.0
-109	.063	149.0
-109	.124	136.0
-109	.187	115.2
-109	.270	113.0
-109	.497	106.5
-109	.650	106.3
70	.033	138.0
70	.140	127.2
70	.187	118.2
70	.252	104.7
70	.522	97.9
70	.624	102.0
550	.030	99.3
550	.065	98.0
550	.138	98.0
550	.378	98.4
550	.578	101.5
AM 350 (20% CRT)		
-109	0.250	180.8
-109	.356	176.9
-109	.546	160.7
70	.046	181.0
70	.066	182.3
70	.124	180.2
70	.181	179.2
70	.250	181.6
70	.381	182.0
70	.500	177.8
70	.625	179.6
550	.034	168.0
550	.072	160.6
550	.131	159.1
550	.169	155.0
550	.264	150.5
550	.488	146.2
550	.591	132.3
AM 350 (double aged)		
-109	0.029	64.9
-109	.129	49.5
-109	.247	47.9
-109	.349	46.7
-109	.603	60.1
70	.031	167.6
70	.062	163.8
70	.129	151.6
70	.189	143.7
70	.261	142.5
70	.379	138.8
70	.513	137.7
70	.634	142.3
550	.034	146.2
550	.070	139.8
550	.111	133.7
550	.137	131.1
550	.262	118.5
550	.343	117.9
550	.501	119.1
550	.629	104.8
PH 15-7Mo (TH 1050)		
-109	0.031	73.6
-109	.125	65.7
-109	.192	49.1
-109	.267	57.0
-109	.382	46.3
-109	.614	45.0
70	.048	[a]181.8
70	.096	[a]151.2
70	.170	[a]125.5
70	.244	133.7
70	.278	137.9
70	.290	132.1
70	.451	132.0
70	.472	126.5
70	.575	132.2
70	.794	144.2
70	.794	146.1
550	.037	175.0
550	.078	162.1
550	.113	145.0
550	.275	127.0
550	.404	120.8
550	.598	110.0
AISI 301 (50% CR)		
-109	0.118	205.4
-109	.263	174.8
-109	.429	162.6
-109	.498	174.3
-109	.625	167.3
70	.063	197.1
70	.141	169.3
70	.187	165.8
70	.226	154.2
70	.380	147.4
70	.510	147.0
70	.676	167.9
550	.029	131.6
550	.058	105.0
550	.117	84.2
550	.121	83.7
550	.276	73.8
550	.378	70.1
550	.503	73.9
550	.619	100.3
René 41 (condition B)		
-109	0.132	128.2
-109	.136	131.2
-109	.169	129.8
-109	.208	115.2
-109	.376	97.3
-109	.563	86.5
70	.034	147.9
70	.061	139.9
70	.125	127.4
70	.198	121.3
70	.379	117.5
550	.041	123.8
550	.125	125.6
550	.238	118.0
550	.394	103.0
550	.498	108.3

[a]Without guides.

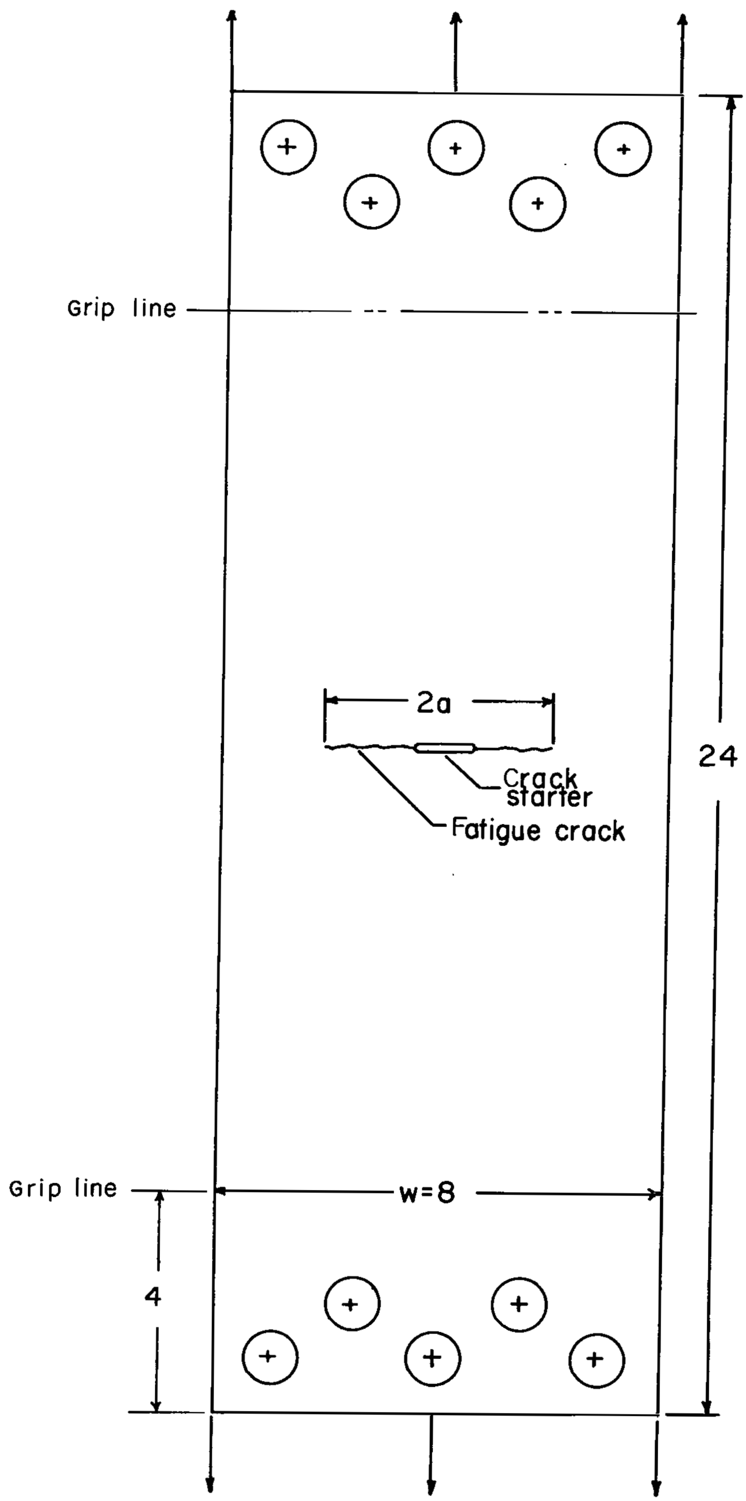

Figure 1.- Specimen configuration. All dimensions are in inches.

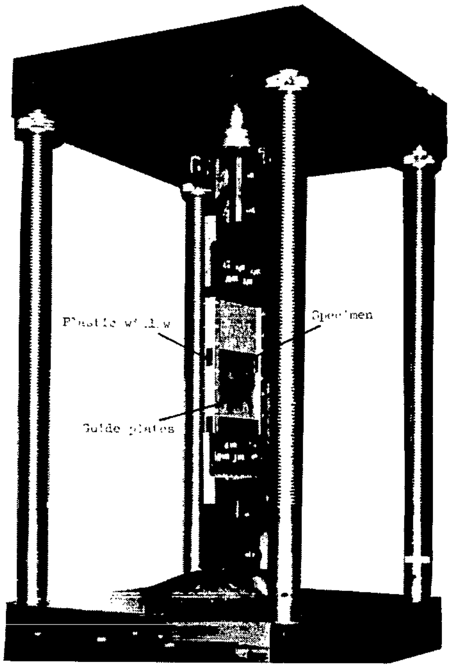

(a) Room temperature.

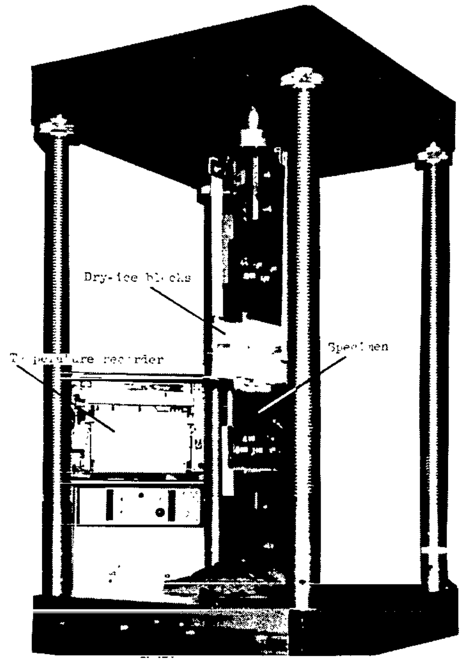

(b) Cryogenic temperature.

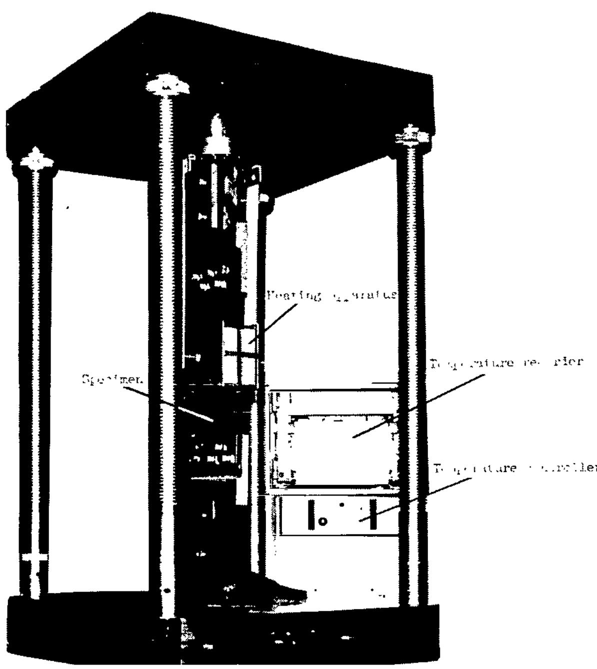

(c) Elevated temperature.

L-63-7511

Figure 2.- Test apparatus.

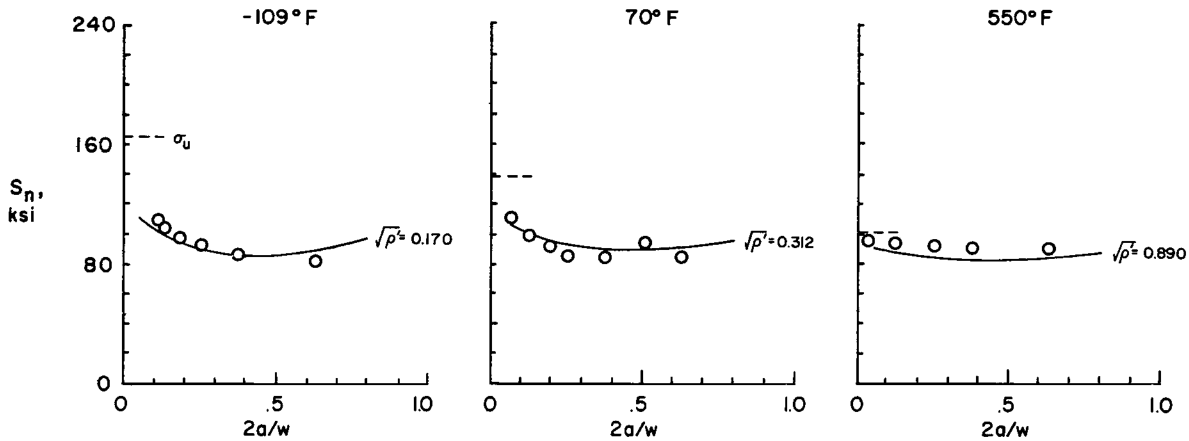

Figure 3.- Residual static strength of Ti-4Al-3Mo-1V (aged) at -109° F, 70° F, and 550° F.

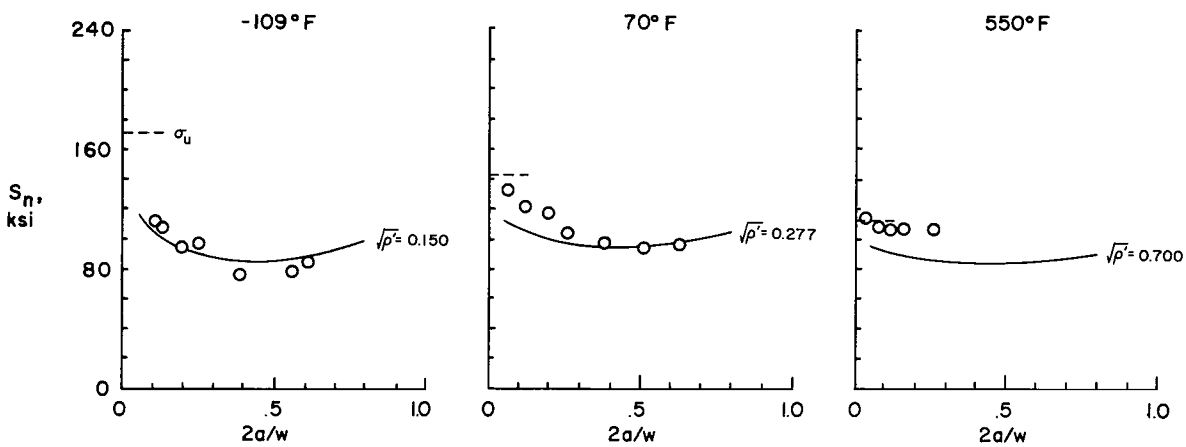

Figure 4.- Residual static strength of Ti-6Al-4V (annealed) at -109° F, 70° F, and 550° F.

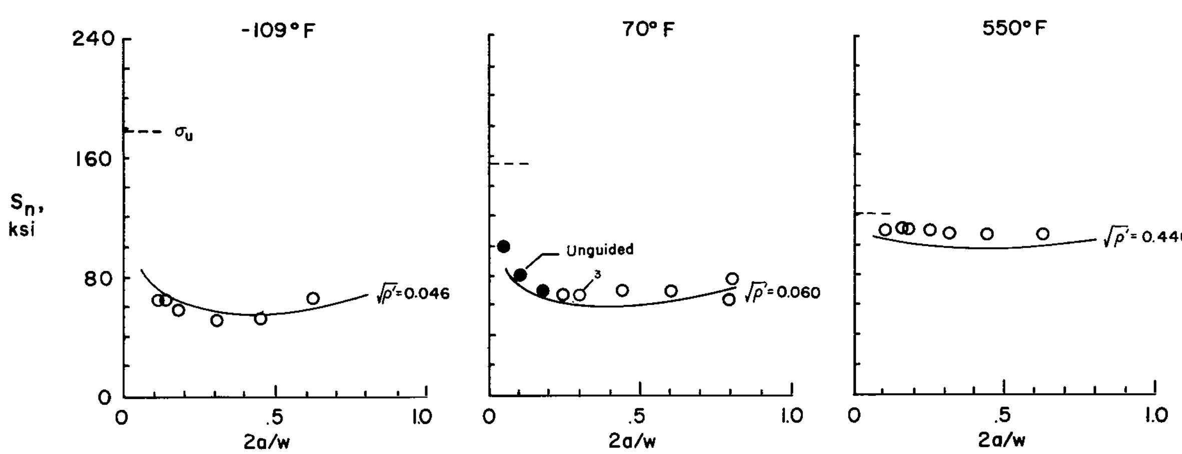

Figure 5.- Residual static strength of Ti-8Al-1Mo-1V (annealed) at -109° F, 70° F, and 550° F.

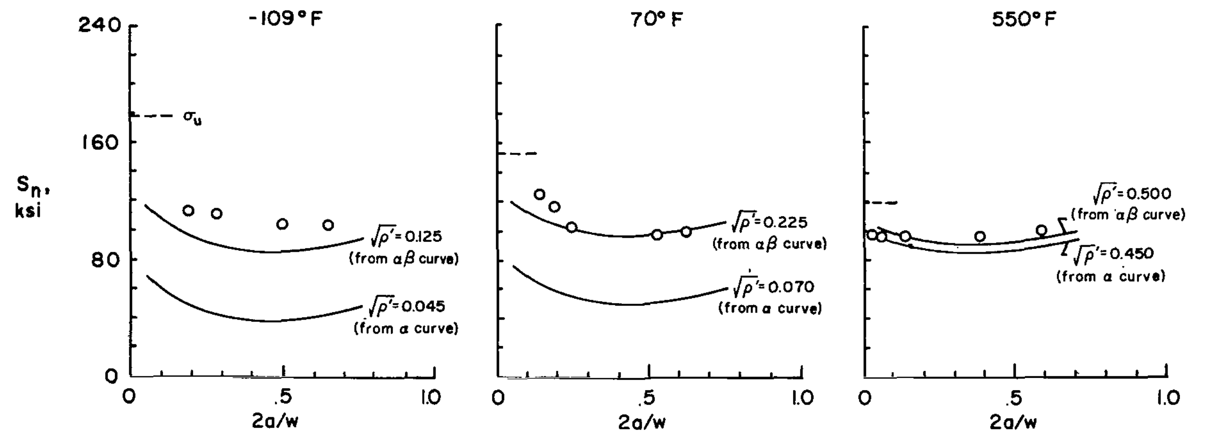

Figure 6.- Residual static strength of Ti-8Al-1Mo-1V (triplex annealed) at -109° F, 70° F, and 550° F.

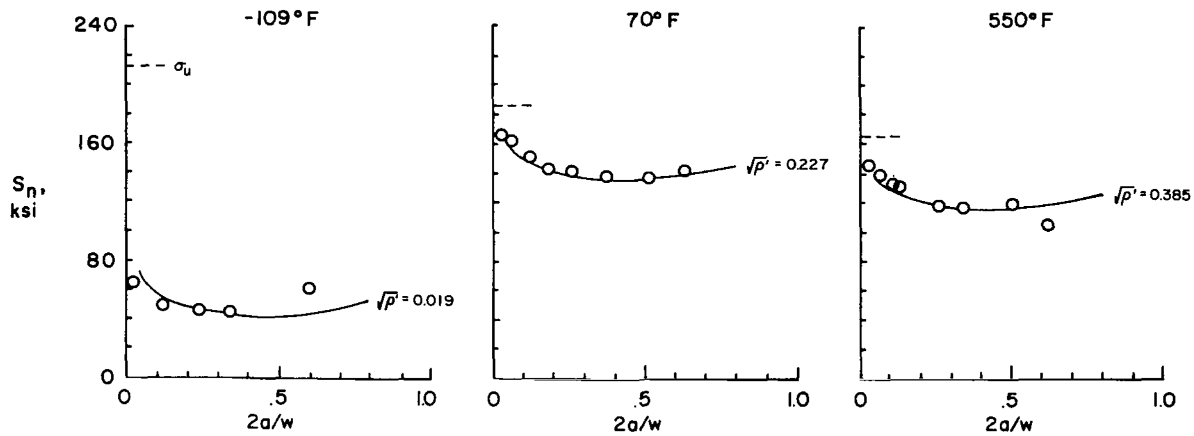

Figure 7.- Residual static strength of AM 350 (double aged) at -109° F, 70° F, and 550° F.

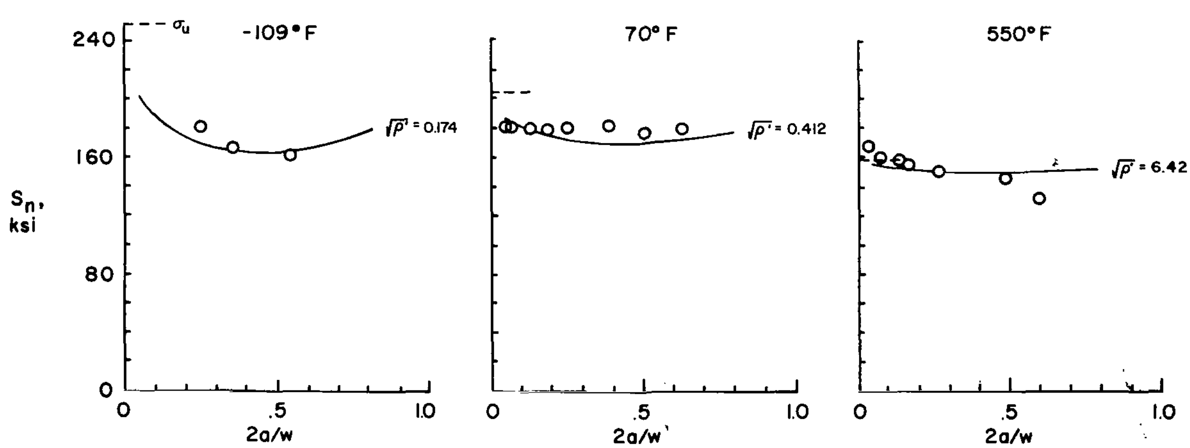

Figure 8.- Residual static strength of AM 350 (20% CRT) at -109° F, 70° F, and 550° F.

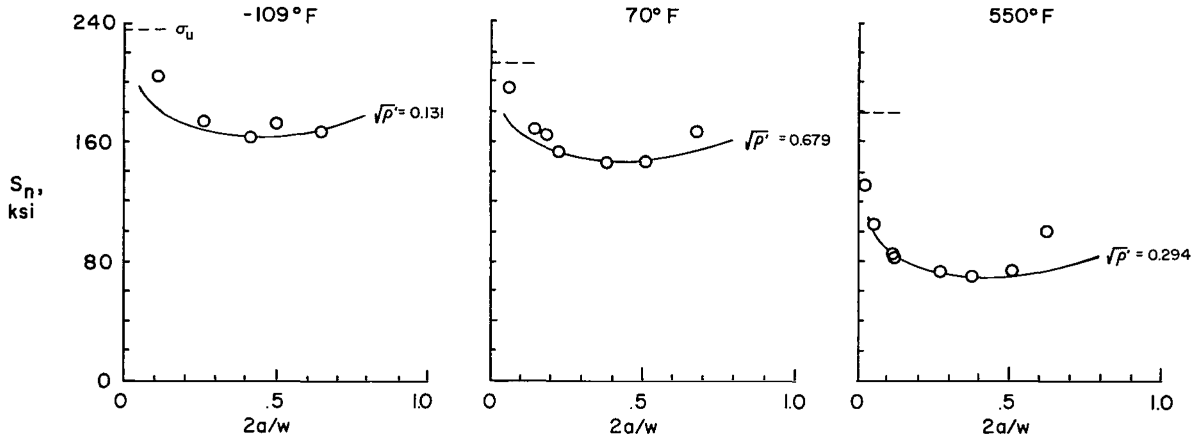

Figure 9.- Residual static strength of AISI 301 (50% CR) at -109° F, 70° F, and 550° F.

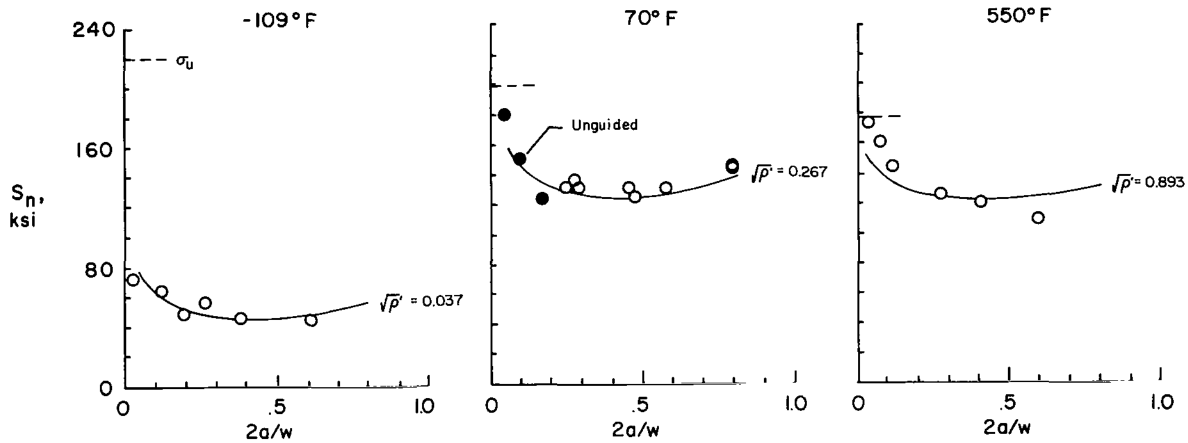

Figure 10.- Residual static strength of PH 15-7Mo (TH 1050) at -109° F, 70° F, and 550° F.

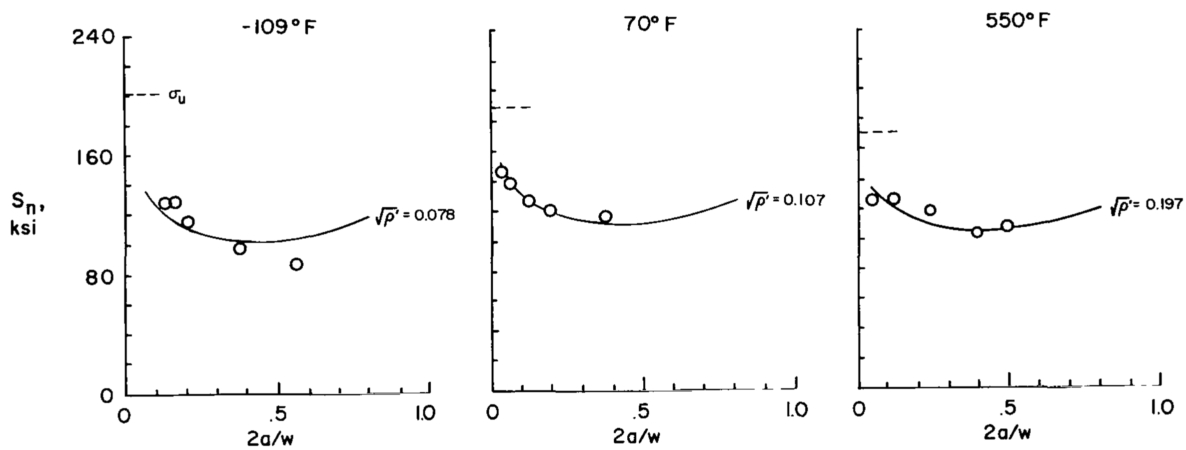

Figure 11.- Residual static strength of René 41 (Condition B) at -109° F, 70° F, and 550° F.

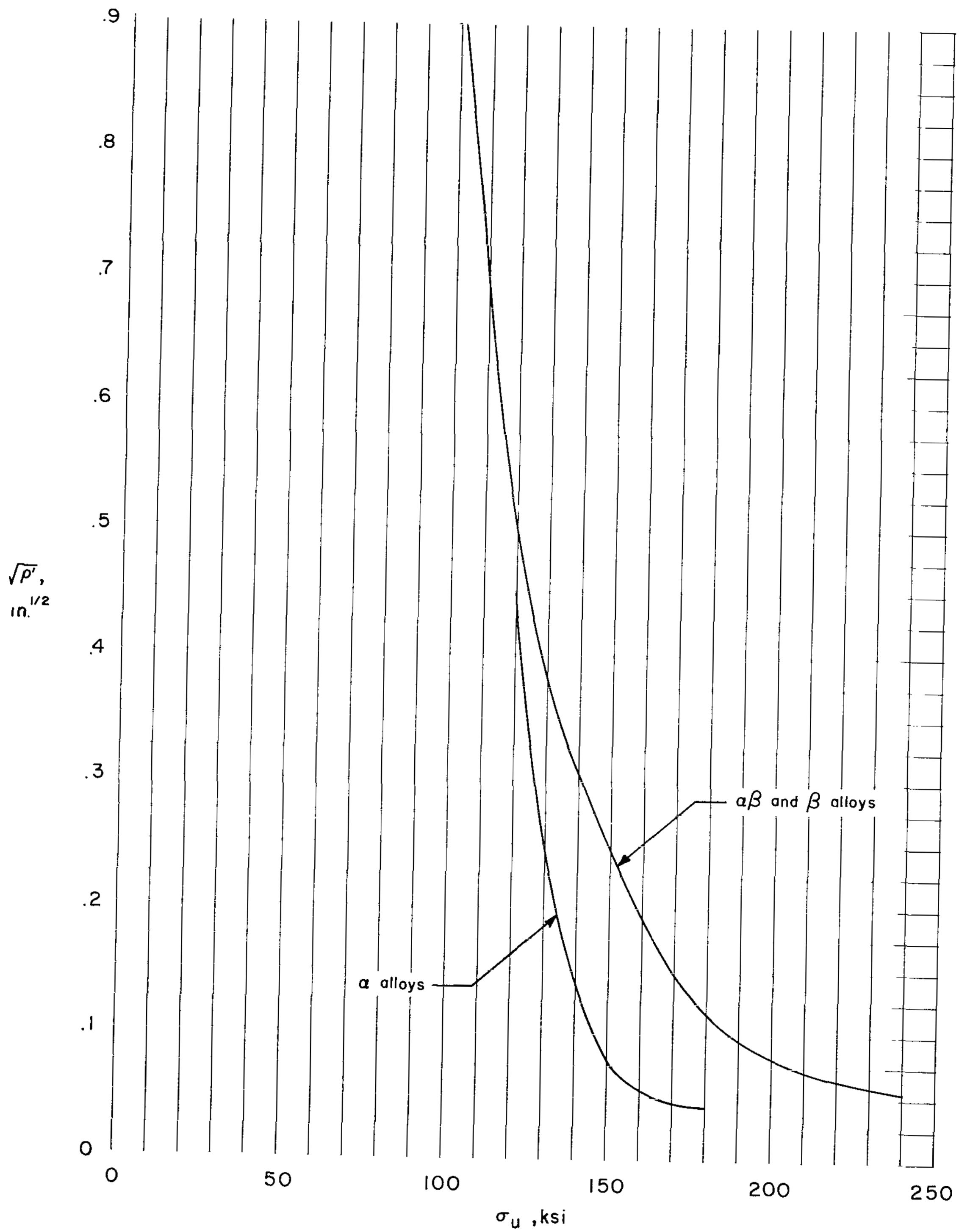

Figure 12.- Tentative Neuber constants for titanium alloys.

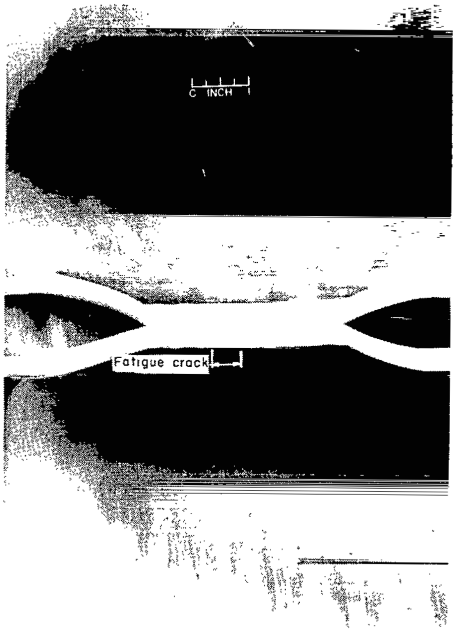

(a) Brittle failure of AM 350 (double aged) at -109° F.

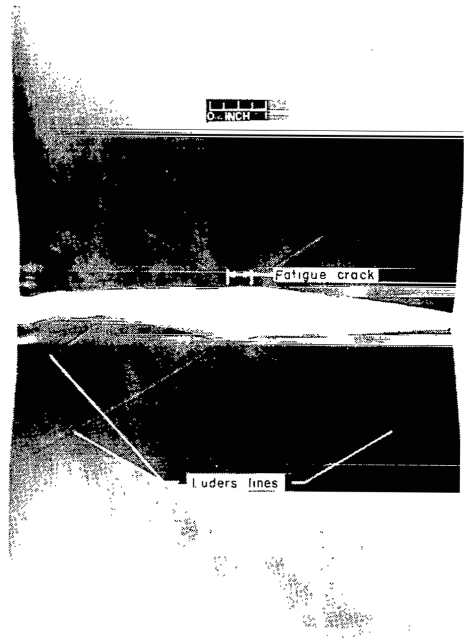

(b) Ductile failure of AM 350 (20% CRT) at 70° F.

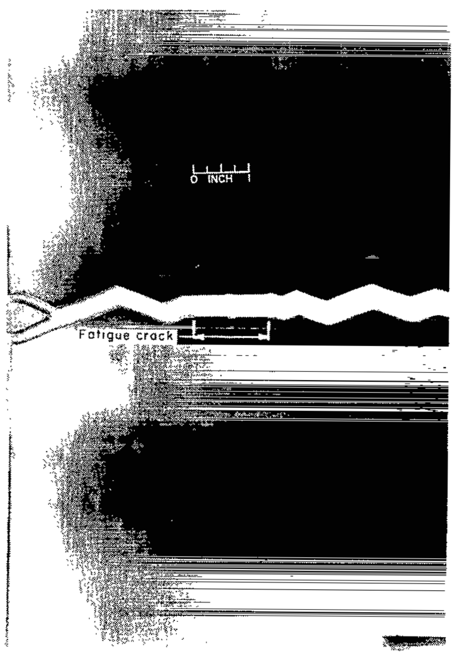

(c) Brittle failure of PH 15-7 Mo (TH 1050) at -109° F.

L-63-7510

Figure 13.- Sheet specimens after static failure.

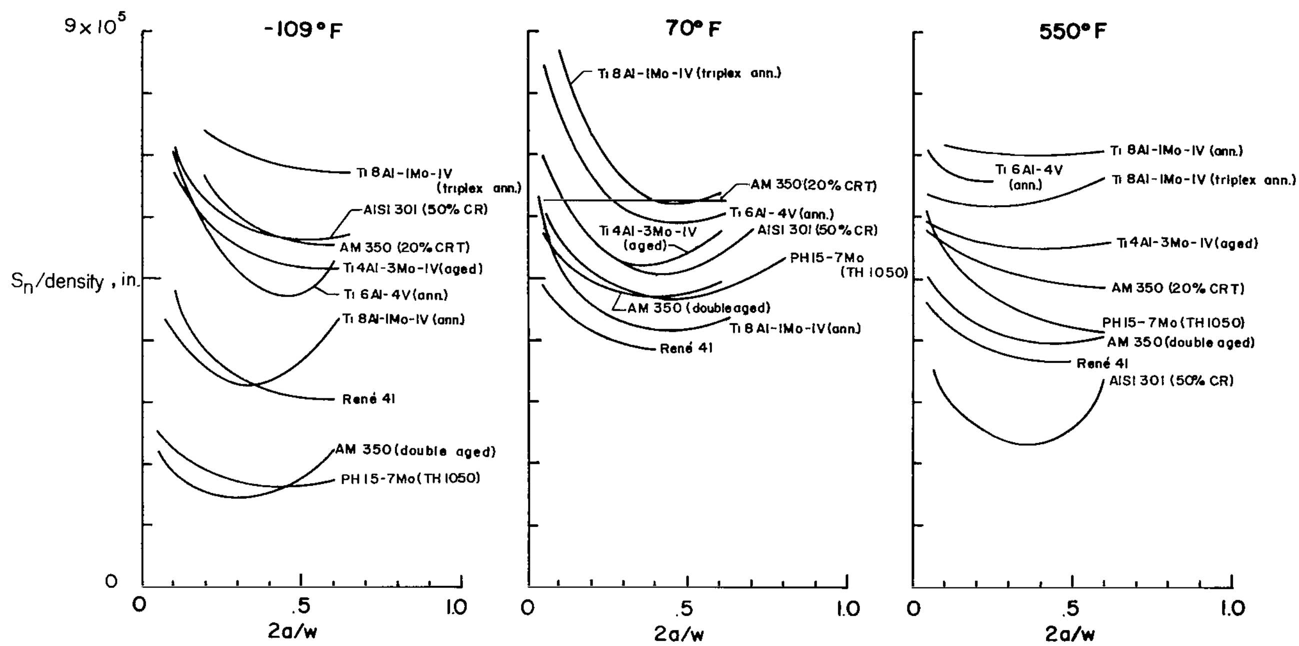

Figure 14.- Variation of residual strength divided by density with 2a/w at -109° F, 70° F, and 550° F.